Bull Mar Sci. 96(1):97–109. 2020
https://doi.org/10.5343/bms.2019.0050

research tools in marine science

A novel low-cost, high-precision sea temperature sensor for coral reef monitoring

James Hendee [1 *]
Natchanon Amornthammarong [1, 2]
Lewis Gramer [1, 2]
Andrea Gomez [3]

[1] *Atlantic Oceanographic and Meteorological Laboratory, National Oceanic and Atmospheric Administration, 4301 Rickenbacker Causeway, Miami, Florida 33149.*

[2] *Cooperative Institute for Marine and Atmospheric Studies, University of Miami, 4600 Rickenbacker Causeway, Miami, Florida 33149.*

[3] *City University of New York, Ecosystem Science Lab-NOAA-CREST, 160 Convent Ave, New York, New York 10031.*

* *Corresponding author email: <jim.hendee@noaa.gov>.*

ABSTRACT.—The role of elevated sea temperatures in coral bleaching has been well documented. Many of the sea temperature records utilized for purposes of widespread, multi-species bleaching predictions in recent publications have been acquired through satellite remote sensing. Satellites estimate sea temperatures at only a narrow range of depths near the surface of the ocean and may therefore not adequately represent the true temperatures endured by the world's coral ecosystems. To better characterize sea temperature regimes that coral reef ecosystems experience, as well as better define the individual thresholds for each species that bleaches, in situ sea temperature sensors are required. Commercial sensors are expensive in large quantities, however, reducing the capacity to conduct large-scale research programs to elucidate the range of significant scales of temperature variability. At the National Oceanic and Atmospheric Administration's (NOAA) Atlantic Oceanographic and Meteorological Laboratory (AOML), we designed a low-cost (roughly US$9 in parts) and high-precision sea temperature sensor that uses an Arduino microprocessor board and a high accuracy thermistor. This new temperature sensor autonomously records temperatures onto a memory chip and provides better accuracy (+0.05 °C) than a comparable commercial sensor (+0.2 °C). Moreover, it is not difficult to build; anyone who knows how to solder can build the temperature sensor. In March 2019, students at middle and high schools in Broward County, Florida, built close to 60 temperature sensors. During 2019, these sensors will be deployed by Reef Check, a global-scale coral reef monitoring organization, as well as by other programs to determine worldwide sea temperature regimes through the Opuhala Project (https://www.coral.noaa.gov/opuhala). This paper chronicles results from the initial proof-of-concept deployments for these AOML-designed sensors.

Date Submitted: 3 April, 2019.
Date Accepted: 16 August, 2019.
Available Online: 19 August, 2019.

The loss of a coral's symbiotic zooxanthellae, or coral "bleaching," through thermal stress (Lesser 1997, Oakley and Davy 2018), as well as other causative factors such as light, is now widely understood by both marine scientists and by those affected by the phenomenon (i.e., fishers, divers, tour operators). Coral researchers have used satellite sea surface temperature measurements and algorithms to predict incidences of bleaching in a proximal way to advise environmental managers and researchers (Hu et al. 2009, Liu et al. 2014). This was done with the hope that they might find better ways to protect fragile coral reef ecosystems from further perturbations.

However, satellites only measure sea temperatures at a narrow, near-surface layer of the ocean (Gentemann and Minnett 2008) and thus may not reliably inform on the effects of sea temperature on benthic organisms. Specifically, satellite data may poorly represent the effects of sea temperature in the molecular ecology involved in coral bleaching, as well as the effect of sea temperature on other aspects of coral ecosystems (e.g., fish and invertebrate spawning, migration, disease, reproduction, etc). Such measurements may be difficult to interpret in light of the underlying environmental causes for temperature variability at coral reefs, for example, the dynamic interplay of wind and ocean currents with ocean heating (Gramer 2013). In situ sea temperature sensors are indicated as the appropriate instrument to answer such questions. Those that are available have proven sufficient for many purposes when instrument spacing and precision are acceptable. Although the use of more precise measurements at a greater spatial density is often desirable, it comes at a greater cost. To address this challenge, we developed a precise, inexpensive sensor to improve the ability to measure and monitor temperatures on coral reefs. The sensor can provide highly accurate measurements that enable researchers to observe temperature variations at multiple locations at reef sites (Fig. 1).

Reef Check Foundation, an international organization dedicated to coral reef monitoring, has expanded its reach over the years to every major coral reef area in the world. It is thus positioned to conduct a global reef sea temperature measurement project not only to inform the measurements made by satellites at wider spatial scales, but also to allow research on the comparative aspects of bleaching of the same taxon between different habitats and in different geographic areas. Such knowledge will hopefully lead to a better understanding of why some colonies of a particular species bleach while others at different locations and under different conditions do not.

Reef Check is typically supported by nongovernmental sources (*see* website at https://reefcheck.org) and lacks the capacity to financially support an intensive global sea temperature monitoring program using commercially available instrumentation. In partnership with Reef Check, the sensor developed at AOML will help to establish the long-term status and trends of coastal sea temperatures, as well as establish a synoptic global picture of reef sea temperatures at a specific time after all sensors have been deployed. This currently developing federal/nongovernmental partnership—termed the Opuhala Project for the ancient Hawaiian goddess of corals and spiny sea creatures—is planned for execution beginning in 2019.

As an initial proof of concept for the use of the sensor in the Opuhala Project, we deployed thirty sensors off the Broward County coastline along the southeast Florida shelf. The present document summarizes the accuracy of the sensors in both our controlled tests and in situ deployments on these reefs. We also demonstrate the

Figure 1. Assembled thermistors arrayed in the lab, ready for deployment.

utility of having access to a large number of low-cost sensors by presenting scientific results which demonstrate the surprisingly fine-scale variability of sea temperatures measured beneath the surface in this particular reef system.

Methods

Water temperature is commonly measured with an electronic device called a thermistor. A thermistor's resistance changes in response to temperature. The relationship between temperature and a thermistor's resistance is highly dependent upon the materials from which it is composed. The manufacturer of the sensor typically determines this property with a high degree of accuracy. Thermistors provide a higher resistance to change per degree of temperature than other kinds of temperature sensors, which results in greater temperature resolution. They also provide a high level of repeatability, stability, and interchangeability. In addition, thermistors are typically smaller than other sensors, which means they quickly respond to temperature changes.

Thermistors differ from Resistance Temperature Detectors (RTDs) in that the material used in a thermistor is typically ceramic or a polymer, while RTDs use pure metals. The temperature response is also different; RTDs are useful over larger temperature ranges, while thermistors typically achieve a greater precision within a limited temperature range (typically −90 °C to 130 °C). To design a low-cost, highly accurate sensor, it is desirable to use a high-quality thermistor. Modern technology has resulted in the production of thermistors with extremely precise resistance versus temperature characteristics that are easy to use, inexpensive, highly sensitive, sturdy, and respond predictably to changes in temperature. Although they do not work well with excessively hot or cold temperatures, they are ideal when precise temperatures are required within a relatively restricted range. The amount by which the resistance decreases as the temperature increases is not constant—it varies in a nonlinear way. A formula called the Steinhart-Hart equation found in the thermistor's datasheet can be used to convert the resistance of the thermistor to temperature:

$$1/\mathrm{T} = A + B(\ln R) + C(\ln R)^3 \qquad \text{Eq. 1}$$

This equation calculates with greater precision the actual resistance [R (Ohms)] of a thermistor as a function of temperature [T (°C)]. Most thermistor manufacturers provide the A, B, and C coefficients for a typical temperature range.

In recent years, there are several ongoing Arduino-based, low-cost data logger projects that have been reported (Gandra et al. 2015, Lockridge et al. 2016, Beddows and Mallon 2018, Parra et al. 2018). However, instruments from these projects cost at least US$20 and are relatively difficult to build, which requires someone who has technician-level skills to build the instruments. Because of the need to produce a large number of sensors for deployment at hundreds of sites, we developed a new, inexpensive (roughly US$9, not including labor and development costs), and high-precision sea temperature logger that uses an Arduino microprocessor board and a high accuracy thermistor. This new temperature sensor autonomously records temperatures onto a memory chip and provides better accuracy (+0.05 °C) than comparable commercial sensors. It can remain submerged for over 4 mo without a change of its two AA batteries. The novelty of the temperature sensor is the combination of its parts that make it such a low-cost and high-precision temperature logger. Currently, there is no underwater temperature sensor that can achieve these goals.

Opuhala Temperature Sensor.—Figure 2 illustrates how the Opuhala temperature sensor works. The temperature sensor can be operated with DC power sources that can generate DC voltage from 1.8 to 5 volts. A step-up 5 V regulator is used to regulate DC voltage from its input (supply) to its output (load). The regulator generates a regulated 5 V output voltage to power the entire system. A high-accuracy thermistor is a thermally sensitive resistor which exhibits a large, predictable, and precise change in electrical resistance when subjected to a corresponding change in body temperature. The thermistor has +0.05 °C interchangeability accuracy, 1 mW/ °C dissipation constant, 30 mW maximum power rating, and 1 s thermal time constant. The electrical resistance of the thermistor is measured using an Arduino Nano microprocessor, which is open-source hardware preprogrammed with a boot loader that simplifies uploading of programs to the on-chip flash memory. Most Arduino boards consist of an Atmel 8-bit Advanced Virtual RISC (AVR) microprocessor with flash memory, pins, and features. They are loaded with program code via Universal Serial Bus (USB), implemented using USB-to-serial adapter chips such as the FTDI FT232. The Arduino Nano is a small, complete, and easy to implement electronics board based on the Atmel 8-bit AVR microprocessor. After reading the electrical resistance to temperature, the Arduino Nano converts the electrical resistance to temperature using the Steinhart-Hart equation. The Arduino Nano then records the temperature onto a memory chip which is a serial, electrically erasable, programmable read-only memory device capable of operation across a broad voltage range (1.7–5.5 V).

Deployment.—A deployment plan for the sensors was developed based on the location of mooring buoys maintained by Broward County, Florida. The number of sensors available allowed for a geographically dense arrangement of the sensors, as well as the placement of a sensor near the top and further down in the water column along each chosen mooring line (Table 1). The accuracy of the sensors enabled us to compare the fine-scale geographic and vertical structure of sea temperatures within

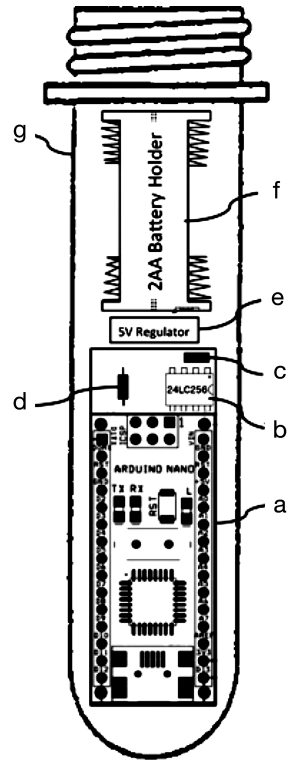

Figure 2. Diagram of the low-cost, high-accuracy and submersible thermistor: (a) Arduino Nano, (b) memory chip, (c) high accuracy thermistor, (d) 10K ohm resistor, (e) step-up 5 V regulator, (f) 2AA battery holder, and (g) PET (Polyethylene terephthalate) preform tube.

Table 1. Information about each temperature sensor deployed in Broward County, Florida.

Mooring Buoy Group Name	NOAA ID for Buoy Location	Latitude (Decimal Degrees)	Longitude (Decimal Degrees)	Depth of Sensor (meters)
Pompano dropoff (north)	PDN1	26.2343	−80.0821	3.5
Pompano	PDN3	26.2264	−80.0828	3.5
Dropoff (north)	PDN2	26.2230	−80.0833	3.7
Pompano	PDS2	26.2072	−80.0851	4.0
Dropoff (north)	PDS1	26.2036	−80.0852	4.1
Anglin's Ledge	AL2	26.1945	−80.0868	4.6
Anglin's Ledge	AL3	26.1935	−80.0868	4.6
Anglin's Ledge	AL1	26.1882	−80.0876	3.7
Anglin's Ledge	AL4	26.1861	−80.0878	4.3
Anglin's Ledge	AL5	26.1840	−80.0880	5.8
Hall of Fame	HF2	26.1935	−80.0843	6.9
Hall of Fame	HF1	26.1921	−80.0849	5.2
Oakland Ridges	OR2	26.1569	−80.0891	6.1
Oakland Ridges	OR1	26.1537	−80.0892	7.8
Caves	CV1	26.1288	−80.0915	6.4
Anglin's Ledge	TCM	26.1935	−80.0866	6.1

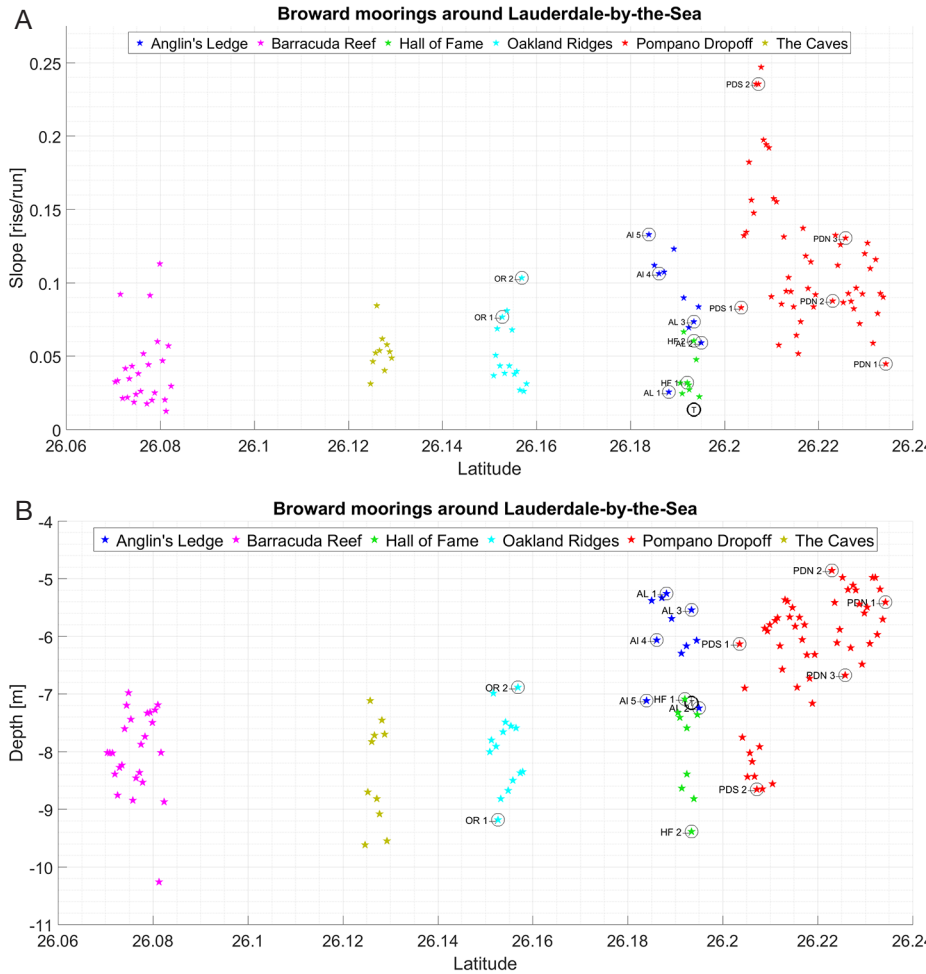

Figure 3. (A) Plots of all Broward County, Florida mooring buoy locations by reef area (colored dots), arranged by latitude (*x*-axis) vs seafloor slope. For details of how seafloor slope was estimated, *see* text. Locations where thermistors were deployed for the present study are circled and labeled in black. (B) Plots of all Broward County, Florida mooring buoy locations by reef area (colored dots), arranged by latitude (*x*-axis) vs seafloor depth. Locations where thermistors were deployed for the present study are circled and labeled in black.

this relatively small area of a reef system. The deployment depths for the deeper sensor on each line were chosen to lie below the expected base of the diurnal warm layer, based on data from previous monitoring on the southeast Florida shelf (Soloviev et al. 2015, Gramer et al. 2018). Particular mooring line locations were chosen to coherently sample (i.e., potentially oversample) the expected horizontal scale of significant sea temperature variability on the shelf. They were also chosen to provide a stratified sampling of temperatures over a variety of water column depths, a variety of distances from the shore and from the deeper waters offshore, and a variety of seafloor slopes (Fig. 3). Site seafloor slope was estimated as the two-point finite difference gradient calculated from a 30-m resolution bathymetry product (Carignan et al. 2015), averaged over three bathymetric gridpoints or approximately 90 m. Consideration of

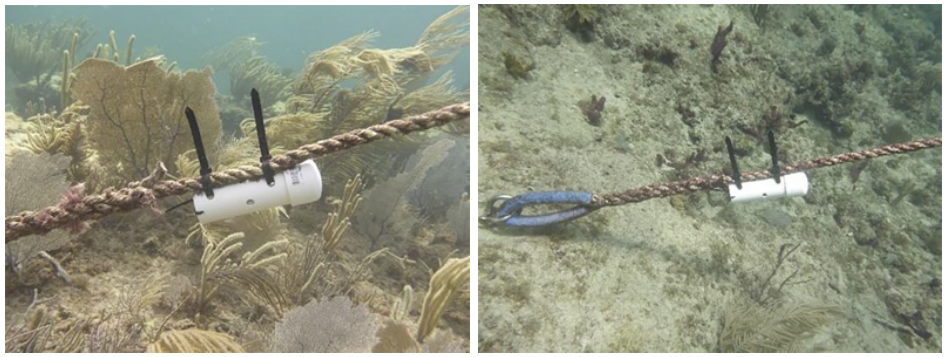

Figure 4. Two examples of PVC in situ deployment packages for near-bottom thermistors.

seafloor slope in the design was based on observations in the Florida Keys and elsewhere that near-bottom sea temperature variability is related to local seafloor slope (Monismith et al. 2006, Gramer 2013, Molina et al. 2014).

On 14 August, 2017, we deployed the Opuhala sensors along the Broward County shelf. The sensors were placed inside PVC pipes for protection and fastened with common commercial cable ties to the boat-mooring lines. Two sensors were deployed at each site, with one sensor being placed about a meter below the sea surface and the other sensor attached near the bottom of the mooring (Fig. 4). We were able to deploy 30 sensors at 15 sites. Sensor depths ranged from about 4.8 to 9.1 m.

Results

Instrument Performance.—In previous tests, the sensors were deployed at different depths at local reef sites (i.e., 9, 14, 21, 30, and 34 m). The sensors for the present study remained in place for approximately 2.5 mo, measuring the sea temperature every 15 min, and then were retrieved to evaluate their performance. A 15-min recording interval was chosen to sample for potential high-frequency variability associated with internal wave breaking or other forcing mechanisms known to operate on other reefs in Florida (Leichter et al. 2005). We found that the PET (polyethylene terephthalate) preform enclosures for the sensors prevented leakage at underwater depths up to 34 m.

In terms of sensitivity, the Opuhala sensor was compared with a HOBO Water Temp Pro v2 temperature sensor (Lentz et al. 2013, Onset Computer Corporation 2019) in a temperature-controlled water bath. Both sensors were dropped into the water bath with the temperature set at 20 °C. The results showed that the HOBO sensor reached the set temperature within 18 min, while the Opuhala sensor reached the target temperature within 14 min.

The Opuhala sensor was calibrated and tested with a certified RTD thermometer (NIST traceable) in a temperature-controlled water bath from 9.2 to 53.8 °C. The results showed a good agreement with a linear coefficient of determination of 1.00 ($y = 1.0014 + 0.0009x$, RMSE = 0.041, $N = 8$).

The Opuhala sensor was also compared along with a HOBO Water Temp Pro v2 sensor in our laboratory and in the field for 2 mo. A high precision laboratory water bath was used for calibrating the two temperature sensors. The results from 2 mo of deployment in the field (Figs. 5, 6) showed a good agreement between these sensors,

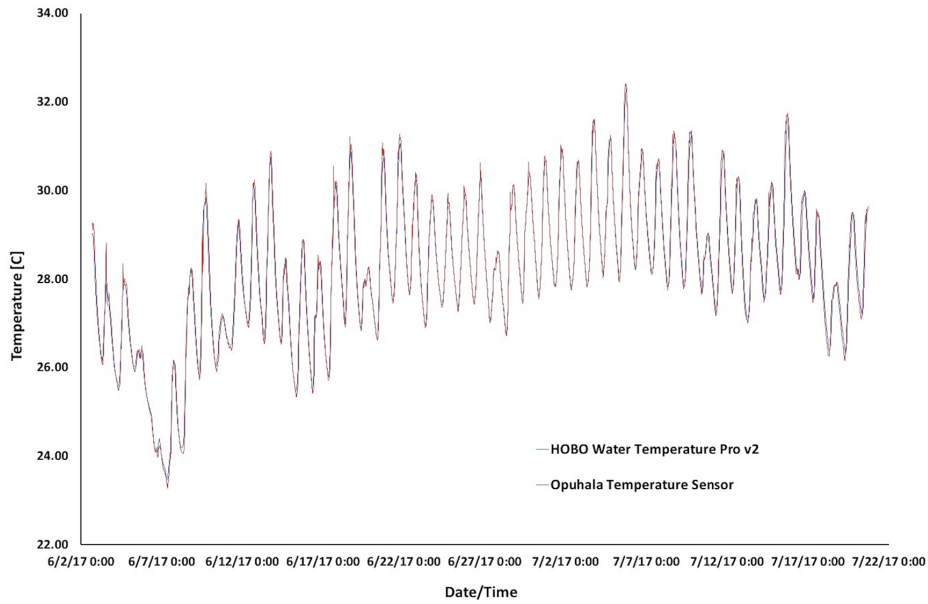

Figure 5. Comparison of sea temperature time series from a calibrated HOBO Water Temp Pro v2 and an Opuhala sensor for about 2 mo.

with a linear coefficient of determination of 0.98 ($y = 1.0007 + 0.0001x$, RMSE = 0.08, $P < 0.01$, $N = 4615$).

With two AA-sized batteries, the Opuhala sensor can be operated about 4 mo while the HOBO sensor can last more than a year with a special type of battery which needs to be sent back to the factory for changing. The reason that the Opuhala sensor consumes more energy is because the Opuhala sensor uses a USB port for

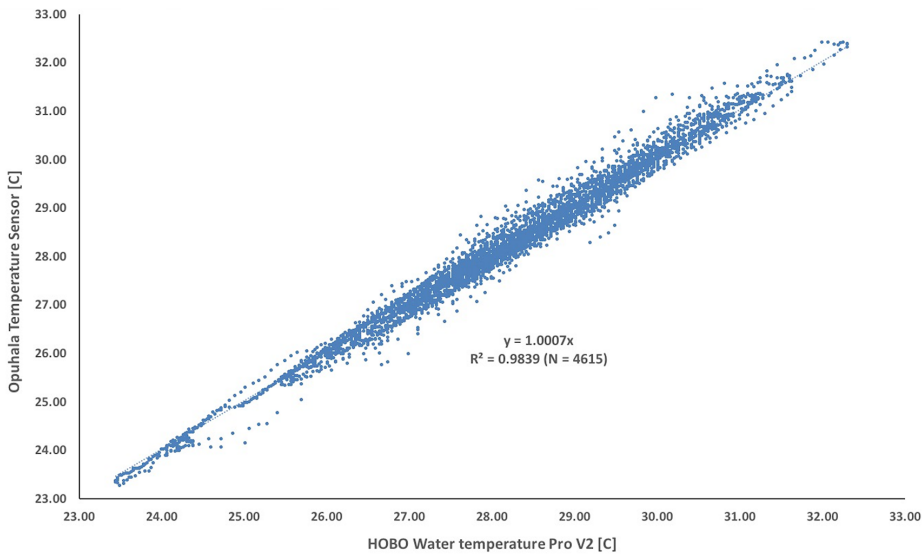

Figure 6. Scatter plot comparing data of the HOBO Water Temp Pro v2 and the Opuhala sensor.

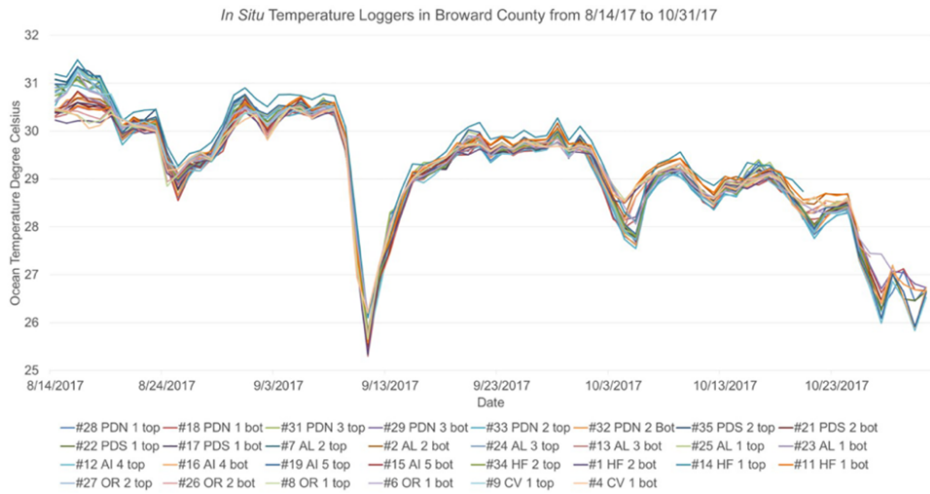

Figure 7. One-day average of nighttime-only in situ temperatures recorded from 14 August, 2017 to 31 October, 2017.

communication. Users only need a typical USB cable and our free software, which can be downloaded at https://www.coral.noaa.gov/opuhala/sensor.html then used to upload the data out of the sensor. Typically, 2–3 mo of deployment will already cause severe biofouling on the sensor, which may affect the accuracy of temperature measurement. Replacing the sensor (a "swap-out") would be an effective and convenient method for field operations to ensure data continuity. In case of a longer deployment in which more than 4 mo are needed, more AA batteries can be easily added or the type of Arduino can be changed from Nano to Pro Mini module, which has no USB port on board. Recently, a new model using Arduino Pro Mini has been developed which can be operated for over a year with two AA-sized batteries. However, a Future Technology Devices International (FTDI) USB to serial cable is needed for interfacing with Arduino Pro Mini.

Nighttime Only Temperatures.—Temperature data were aggregated into nighttime only daily values from 14 August, 2017 to 31 October, 2017 (Fig. 7). To produce these time series, the set of all 15-min samples for each site that occurred between local sunset and local sunrise on each night were averaged together. All of these nighttime-only average time series followed a similar pattern, with little variation between sites.

Hurricane Irma impacted Florida on 10 September, 2017, and the dramatic temperature decrease was chronicled by all in situ loggers. Temperatures dropped by about 5 °C due to the hurricane (from approximately 30.5 °C to approximately 25.5 °C). After almost a week, temperatures started to rise, but then decreased in late September/early October.

Temperature Gradients.—In terms of geographic differences, coincident temperatures at the different deployment sites showed a wide range of daytime temperature extremes, particularly early in the record in August 2017 (Table 2). Median values for the 1681 quarter-hourly samples gathered in August, including all hours of

Table 2. Statistics for each top and bottom sensor (median, max, min, and interquartile range).

NOAA ID (dates collected)	Median	Maximum	Minimum	Interquartile
PDN1 top (08/14–10/31)	29.24	31.07	25.67	1.46
PDN1 bot (08/14–10/31)	29.24	30.60	25.54	1.55
PDN3 top (08/14–10/24)	29.47	31.05	25.60	1.34
PDN3 bot (08/14–10/31)	29.32	30.67	25.48	1.48
PDN2 top (08/14–10/27)	29.27	30.97	25.43	1.39
PDN2 bot (08/14–10/31)	29.27	30.68	25.46	1.52
PDS2 top (08/14–08/24)	30.58	31.31	29.51	0.84
PDS2 bot (08/14–10/28)	29.39	30.60	25.54	1.34
PDS1 top (08/14–10/31)	29.21	31.13	25.61	1.43
PDS1 bot (08/14–10/24)	29.40	30.59	25.58	1.29
AL2 top (08/14–09/29)	29.83	31.34	25.64	1.15
AL2 bot (08/14–10/26)	29.50	30.70	25.33	1.19
AL3 top (08/14–10/25)	29.43	31.24	25.52	1.41
AL3 bot (08/14–10/22)	29.44	30.55	25.30	1.12
AL1 top (08/14–10/27)	29.46	31.32	25.61	1.44
AL1 bot (08/14–09/09)	30.34	30.83	28.98	0.58
AI4 top (08/14–10/31)	29.17	31.30	25.57	1.53
AI4 bot (08/14–10/31)	29.32	30.79	25.50	1.46
AI5 top (08/14–10/31)	29.28	31.34	25.64	1.48
AI5 bot (08/14–09/24)	29.93	30.83	25.50	1.09
HF2 top (08/14–10/26)	29.35	31.14	25.83	1.40
HF2 bot (08/14–10/18)	29.52	30.54	25.33	1.01
HF1 top (08/14–10/20)	29.80	31.49	26.09	1.22
HF1 bot (08/14–10/24)	29.54	30.72	25.58	1.11
OR2 top (08/14–09/09)	30.36	31.23	29.07	0.47
OR2 bot (08/14–10/26)	29.41	30.53	25.75	1.11
OR1 top (08/14–10/24)	29.46	30.49	25.65	1.14
OR1 bot (08/14–10/28)	29.37	31.23	26.20	1.36
CV1 top (08/14–09/09)	30.32	31.24	29.24	0.54
CV1 bot (08/14–10/25)	29.44	30.48	26.20	1.16

the day, differed by up to 0.6 °C between sites (*see* analysis below). A one-way ANOVA showed two moorings with near-surface temperature means significantly higher in August than the others [site HF1 with a mean of 30.46 and site PDS2 with a mean of 30.67 ($N = 1681$, $P < 0.0001$)]. August medians at other sites ranged from 29.92 to 30.31. A similar analysis for the months of September and October 2017 ($N = 2880$ and 2976, respectively; $P < 0.0001$) showed multiple, distinct outlier sites for each of these months as well, despite the obvious region-wide effects of Hurricane Irma in September and of other, more remote, tropical weather systems such as Hurricane Nate in October (Fig. 8).

Considering vertical gradients, differences in temperature between the near-surface and near-bottom thermistors were also significant (*see* analysis below, $P < 0.05$ for all comparisons), both during the doldrum warming period of late August (Atwood et al. 1992), during the most extreme cooling effects of Hurricane Irma in September 2017, and during events in October and November 2017 (Fig. 8). During multiday periods on 15–20 August ($N = 577$) and from 29 August to 4 September ($N = 672$), when nearby meteorological monitoring stations recorded low winds (daily average 10-m

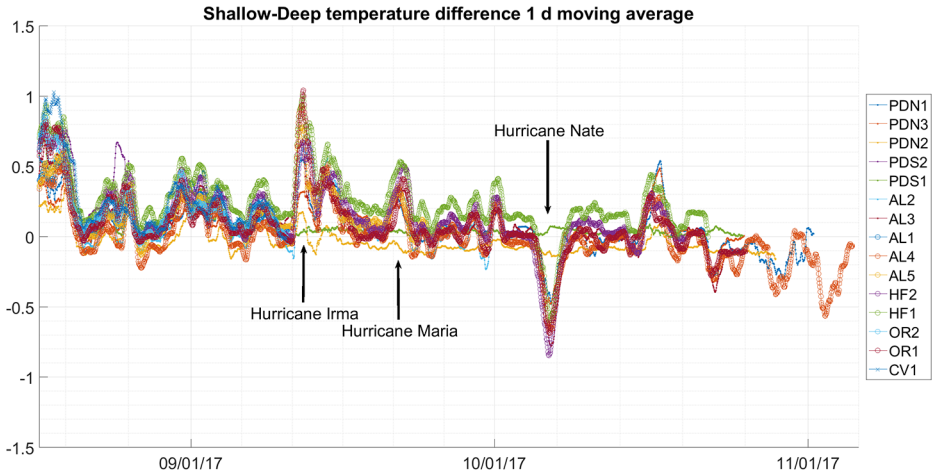

Figure 8. Simple moving daily average differences between near-surface and near-bottom thermistors at each site, including both day and night values. The closest approach of hurricanes Irma, Maria, and Nate is highlighted in black.

winds of 10 knots or less at Fowey Rocks Lighthouse and Port Everglades), the daily average difference between top and bottom sensors at each site was greater than +0.1 °C. At some sites in August, including CV1 and HF1, it remained between +0.8 and +1.1 °C for a full day or more. Finally, as discussed further below, daily averages for near-bottom sea temperatures at several sites around 4 October were 0.4–0.8 °C higher than those near the surface at the same site, for example, at HF1.

Discussion

The Opuhala sensor can provide better precision at a much lower cost than the HOBO Water Temp Pro v2, which costs about 12 times more. The Opuhala sensor is not difficult to build; new design considerations for the Opuhala sensor include a goal of being able to deploy it at depths greater than 34 m, the capability to transfer data underwater via infrared communication, and the addition of other sensors to the sensor package (e.g., pH, pressure, light, conductivity). The low cost of materials for the sensor, coupled with its measurement accuracy, will enable new science to be conducted which would not be possible otherwise.

Results for nighttime-only temperature averages showed close agreement across all sites. This suggests that satellite products based on similar nighttime-only methodologies (e.g., Coral Reef Watch, Liu et al. 2014) may not benefit significantly from increasing spatial resolution. The results when both day and night measurements were included, however, suggests that such satellite methodologies may be significantly improved from both the use of full-day measurements, and from means of estimating subsurface temperature evolution (Gentemann et al. 2009).

Regarding the impact of ocean dynamics on temperature, top-bottom daily average differences at some sites during the 12–72 hrs immediately following the peak winds of Hurricane Irma suggest that part of the observed cooling near the bottom may have been because those winds were favorable to oceanic upwelling. By contrast, during the passage of the more distant tropical weather system Hurricane

Nate around 4 October, daily averages for near-bottom sea temperatures at several sites were 0.4–0.8 °C higher than those near the surface, for example, at HF1. This significant temperature inversion would suggest that these winds were favorable to downwelling, potentially bringing saltier offshore water onto these sites at depth.

The spatial scales of significant variability in sea temperature that have been observed on coral reefs are often less than 1 km (Leichter et al. 2006, Gramer 2013, Safaie et al. 2018). This suggests that these environments may need to be much more densely instrumented if we wish to fully understand some of the biological processes that occur on reefs, including coral bleaching (Safaie et al. 2018). The results from the present study bear this out for at least one reef region. Factory calibration and tank tests, presented here, tell us that the between-site differences seen in these data represent real in-water differences; pre- and postcalibration efforts currently being tested for the Opuhala sensors will also be critical in establishing the scales of significant variability in reef temperatures for future studies. Similar considerations of fine-scale spatial and temporal variability also apply to other aspects of the dynamic physical habitat on reefs, including light attenuation (Barnes et al. 2013), sedimentation (Pomeroy et al. 2018), and carbon chemistry (Lubarsky et al. 2018, Murgulet et al. 2018). The low cost and high accuracy of this new sensor design provides the capability to deploy dozens or hundreds of accurate sensors within a coral reef area, thus increasing the reach of science under a reduced budget.

Acknowledgments

The authors would like to thank would like to thank P Fletcher of Broward College, G Hodgson of Reef Check and K Shein, M Eakin, I Enochs, and D Manzello of NOAA for their valuable contributions to the development of the sensor, their critique of the manuscript, and/or and the inception of this study. We also owe a debt of gratitude to G Derr of AOML for her careful attention to details of editing and graphics. This project is funded by NOAA/AOML's Coral Health and Monitoring Program.

Literature Cited

Atwood DK, Hendee JC, Mendez A. 1992. An assessment of global warming stress on Caribbean coral reef ecosystems. Bull Mar Sci. 51(1):118–130.

Barnes BB, Hu C, Schaeffer BA, Lee Z, Palandro DA, Lehrter JC. 2013. Modis-derived spatiotemporal water clarity patterns in optically shallow Florida Keys waters: a new approach to remove bottom contamination. Remote Sens Environ. 134:377–391. https://doi.org/10.1016/j.rse.2013.03.016

Beddows PA, Mallon EK. 2018. Cave pearl data logger: a flexible arduino-based logging platform for long-term monitoring in harsh environments. Sensors (Basel). 18(2):E530. https://doi.org/10.3390/s18020530

Carignan KS, McLean SJ, Eakins BW, Beasley L, Love MR, Sutherland M. 2015. Digital elevation model of Miami, Florida: procedures, data sources, and analysis. Boulder, CO: National Geophysical Data Center.

Gandra M, Seabra R, Lima FP. 2015. A low-cost, versatile data logging system for ecological applications. Limnol Oceanogr Methods. 13(3):115–126. https://doi.org/10.1002/lom3.10012

Gentemann CL, Minnett PJ. 2008. Radiometric measurements of ocean surface thermal variability. J Geophys Res Oceans. 113 C8:13.

Gentemann CL, Minnett PJ, Sienkiewicz J, DeMaria M, Cummings J, Jin Y, Doyle JD, Gramer L, Barron CN, Casey KS, et al. 2009. Misst: The multi-sensor improved sea surface temperature project. Oceanography (Wash DC). 22(2):76–87. https://doi.org/10.5670/oceanog.2009.40

Gramer LJ. 2013. The dynamics of sea temperature variability on Florida's reef tract. [Miami, FL]: University of Miami Rosenstiel School of Marine and Atmospheric Science.

Gramer LJ, Hendee JC, Stamates SJ, Walker BK, Walter RK, Coleman DJ. 2018. Upwelling on the southeast Florida shelf: summer sea temperature extremes and associated nutrient fluxes over a 17 year period. Miami, FL, USA: NOAA AOML.

Hu CM, Muller-Karger F, Murch B, Myhre D, Taylor J, Luerssen R, Moses C, Zhang CY, Gramer L, Hendee J. 2009. Building an automated integrated observing system to detect sea surface temperature anomaly events in the Florida Keys. IEEE Trans Geosci Remote Sens. 47(7):2071–2084. https://doi.org/10.1109/TGRS.2009.2024992

Leichter JJ, Deane GB, Stokes MD. 2005. Spatial and temporal variability of internal wave forcing on a coral reef. J Phys Oceanogr. 35(11):1945–1962. https://doi.org/10.1175/JPO2808.1

Leichter JJ, Helmuth B, Fischer AM. 2006. Variation beneath the surface: quantifying complex thermal environments on coral reefs in the Caribbean, Bahamas and Florida. J Mar Res. 64(4):563–588. https://doi.org/10.1357/002224006778715711

Lentz SJ, Churchill JH, Marquette C, Smith J. 2013. Evaluation and recommendations for improving the accuracy of an inexpensive water temperature logger. J Atmos Ocean Technol. 30(7):1576–1582. https://doi.org/10.1175/JTECH-D-12-00204.1

Lesser MP. 1997. Oxidative stress causes coral bleaching during exposure to elevated temperatures. Coral Reefs. 16(3):187–192. https://doi.org/10.1007/s003380050073

Liu G, Heron SF, Eakin CM, Muller-Karger FE, Vega-Rodriguez M, Guild LS, De La Cour JL, Geiger EF, Skirving WJ, Burgess TFR, et al. 2014. Reef-scale thermal stress monitoring of coral ecosystems: new 5-km global products from NOAA Coral Reef Watch. Remote Sens. 6(11):11579–11606. https://doi.org/10.3390/rs61111579

Lockridge G, Dzwonkowski B, Nelson R, Powers S. 2016. Development of a low-cost arduino-based sonde for coastal applications. Sensors (Basel). 16(4):E528. https://doi.org/10.3390/s16040528

Lubarsky KA, Silbiger NJ, Donahue MJ. 2018. Effects of submarine groundwater discharge on coral accretion and bioerosion on two shallow reef flats. Limnol Oceanogr. 63(4):1660–1676. https://doi.org/10.1002/lno.10799

Molina L, Pawlak G, Wells JR, Monismith SG, Merrifield MA. 2014. Diurnal cross-shore thermal exchange on a tropical forereef. J Geophys Res Oceans. 119(9):6101–6120. https://doi.org/10.1002/2013JC009621

Monismith SG, Genin A, Reidenbach MA, Yahel G, Koseff JR. 2006. Thermally driven exchanges between a coral reef and the adjoining ocean. J Phys Oceanogr. 36(7):1332–1347. https://doi.org/10.1175/JPO2916.1

Murgulet D, Trevino M, Douglas A, Spalt N, Hu XP, Murgulet V. 2018. Temporal and spatial fluctuations of groundwater-derived alkalinity fluxes to a semiarid coastal embayment. Sci Total Environ. 630:1343–1359. https://doi.org/10.1016/j.scitotenv.2018.02.333

Oakley C, Davy S. 2018. Cell biology of coral bleaching. *In*: van Oppen M, Lough J, editors. Coral bleaching. Springer Cham. p. 189–211.

Onset Computer Corporation. 2019[Internet]. Available from: https//www.onsetcomp.com/products/data-loggers/u22-001

Parra L, Lloret G, Lloret J, Rodilla M. 2018. Physical sensors for precision aquaculture: a review. IEEE Sens J. 18(10):3915–3923. https://doi.org/10.1109/JSEN.2018.2817158

Pomeroy AWM, Lowe RJ, Ghisalberti M, Winter G, Storlazzi C, Cuttler M. 2018. Spatial variability of sediment transport processes over intratidal and subtidal timescales within a fringing coral reef system. J Geophys Res Earth Surf. 123(5):1013–1034. https://doi.org/10.1002/2017JF004468

Safaie A, Silbiger NJ, McClanahan TR, Pawlak G, Barshis DJ, Hench JL, Rogers JS, Williams GJ, Davis KA. 2018. High frequency temperature variability reduces the risk of coral bleaching. Nat Commun. 9:12.

Soloviev A, Dean CW, Weisberg RH, Luther ME, Wood J. 2015. ADCP mooring system on the southeast florida shelf. NSU Marine and Environmental Science Reports. Avialable from: https://nsuworks.nova.edu/occ_facreports/52.